The FASEB Journal • Research Communication

Determination of the substrate repertoire of ADAMTS2, 3, and 14 significantly broadens their functions and identifies extracellular matrix organization and TGF-β signaling as primary targets

Mourad Bekhouche,*,[1],[2] Cedric Leduc,*,[1] Laura Dupont,* Lauriane Janssen,*
Frederic Delolme,[†],[‡] Sandrine Vadon-Le Goff,[†] Nicolas Smargiasso,[§] Dominique Baiwir,[¶]
Gabriel Mazzucchelli,[§] Isabelle Zanella-Cleon,[‡] Johanne Dubail,*,[3] Edwin De Pauw,[§]
Betty Nusgens,* David J. S. Hulmes,[†] Catherine Moali,[†],[4] and Alain Colige*,[2],[4]

*Laboratory of Connective Tissues Biology, [§]Mass Spectrometry Laboratory, GIGA Proteomics, and
[¶]GIGA Proteomic Facility, GIGA–Interdisciplinary Cluster for Applied Genoproteomics, University of
Liège, Liège, Belgium; [†]Tissue Biology and Therapeutic Engineering, Centre National de la Recherche
Scientifique/University of Lyon Unité Mixte de Recherche 5305, Lyon, France; and [‡]Protein Science
Facility, Institute for the Biology and Chemistry of Proteins, Unité Mixte de Service 3444, Lyon, France

ABSTRACT   A disintegrin and metalloproteinase with thrombospondin type I motif (ADAMTS)2, 3, and 14 are collectively named procollagen *N*-proteinases (pNPs) because of their specific ability to cleave the aminopropeptide of fibrillar procollagens. Several reports also indicate that they could be involved in other biological processes, such as blood coagulation, development, and male fertility, but the potential substrates associated with these activities remain unknown. Using the recently described N-terminal amine isotopic labeling of substrate approach, we analyzed the secretomes of human fibroblasts and identified 8, 17, and 22 candidate substrates for ADAMTS2, 3, and 14, respectively. Among these newly identified substrates, many are components of the extracellular matrix and/or proteins related to cell signaling such as latent TGF-β binding protein 1, TGF-β RIII, and dickkopf-related protein 3. Candidate substrates for the 3 ADAMTS have been biochemically validated in different contexts, and the implication of ADAMTS2 in the control of TGF-β activity has been further demonstrated in human fibroblasts. Finally, the cleavage site specificity was assessed showing a clear and unique preference for nonpolar or slightly hydrophobic amino acids. This work shows that the activities of the pNPs extend far beyond the classically reported processing of the aminopropeptide of fibrillar collagens and that they should now be considered as multilevel regulators of matrix deposition and remodeling.—Bekhouche, M., Leduc, C., Dupont, L., Janssen, L., Delolme, F., Vadon-Le Goff, S., Smargiasso, N., Baiwir, D., Mazzucchelli, G., Zanella-Cleon, I., Dubail, J., De Pauw, E., Nusgens, B., Hulmes, D. J. S., Moali, C., Colige, A. Determination of the substrate repertoire of ADAMTS2, 3, and 14 significantly broadens their functions and identifies extracellular matrix organization and TGF-β signaling as primary targets. *FASEB J.* 30, 000–000 (2016). www.fasebj.org

Key Words: *N-TAILS* · *betaglycan* · *LTBP1* · *DKK3*

Extracellular matrix (ECM) remodeling is a crucial step in many pathophysiological events such as development, wound healing, fibrosis, and cancer. This complex and well-orchestrated process is constantly regulated through a dynamic crosstalk between cells and their environment. Extracellular proteinases and their respective networks are essential to this process through the degradation of matrix components, release of trapped cytokines and growth factors, generation of cryptic bioactive peptides from larger molecules, and maturation of procollagens. Fibrillar collagens are the most abundant proteins in connective tissues. They are synthesized as trimeric procollagen molecules encompassing the typical central triple-helical domain and terminal propeptides at each extremity. The cleavage of these N- and C-terminal propeptides is required to allow the spontaneous assembly of mature trimers into perfectly organized collagen fibrils and fibers. The procollagen *N*-proteinases (pNPs), a disintegrin and

Abbreviations: ADAMTS, a disintegrin and metalloproteinase with thrombospondin type I motif; ATOMS, amino-terminal–oriented mass spectrometry of substrate; BiNGO, Biological Networks Gene Ontology; BMP, bone morphogenetic protein; CP-III, C-propeptide of procollagen III; CTGF, connective tissue growth factor; DF, dermatosparactic fibroblast;
(continued on next page)

metalloproteinase with thrombospondin type I motif (ADAMTS) 2, 3, and 14, are principally known for their ability to cleave the aminopropeptide of fibrillar collagen precursors (types I, II, III, and V) (1). The critical role of ADAMTS2 in this process is illustrated in the dermatosparactic type of Ehlers-Danlos syndrome, a genetic disease caused by mutations in the *Adamts2* gene. In the absence of ADAMTS2 activity, pN-procollagen (collagen still retaining its N-terminal extension) accumulates, leads to the formation of highly disorganized collagen fibers, and ultimately, causes the extreme skin fragility that is the hallmark of the disease (2).

Additional reports showing the sterility of *Adamts2*-deficient male mice (3), expression of ADAMTS2 by macrophages (4), and recently described genetic association between the *Adamts2* gene and pediatric stroke (5) indicate that the functions and substrate repertoire of ADAMTS2 are probably not limited to fibrillar procollagens. Other genetic studies have linked the *Adamts14* gene to a predisposition to multiple sclerosis (6) or female knee osteoarthritis (7, 8), and the expression of ADAMTS2 and 3 was also shown to be increased in culprit plaques from patients presenting with acute myocardial infarction *vs.* stable angina (9). Finally, it was recently shown that ADAMTS3 is capable of cleaving and activating pro-VEGF-C in experimental models (10). Taken together, these reports suggest that this subfamily of ADAMTS enzymes has functions that are not related to collagen biology, and this prompted us to search additional potential substrates. We used a proteome-wide strategy, named terminal amine isotopic labeling of substrates (TAILS), which specifically identifies the natural N termini of proteins together with the N termini of their cleavage products (11). This approach was successfully used to identify novel substrates of matrix metalloproteinases (MMPs) (12), meprins α and β (13), but has not yet been applied so far to ADAMTS proteinases.

This study aimed at the identification of new substrates of ADAMTS2, 3, and 14. The rationale for studying these 3 ADAMTS in parallel was to increase the likelihood of identifying new substrates of these highly similar enzymes and to better evaluate the extent to which they have overlapping functions. Tens of new substrates were identified, many of them being ECM components and/or regulators of the Wnt or TGF-β pathways, such as latent TGF-β binding protein (LTBP)1 and TGF-β RIII. Additional characterizations confirmed the reliability of the TAILS approach to identify new substrates and demonstrated the functional significance of ADAMTS2 for TGF-β signaling.

(continued from previous page)

DKK, dickkopf-related protein; dpc, days postconception; ECM, extracellular matrix; HEK, human embryonic kidney; HEPES, 4-(2-hydroxyethyl)-1-piperazineethanesulfonic acid; HLA, human leukocyte antigen; iTRAQ, isobaric tag for relative and absolute quantitation; LAP, latency-associated peptide; LLC, large latent complex; LTBP, latent TGF-β binding protein; MEF, mouse embryonic fibroblast; mini-III, miniprocollagen III; MMP, matrix metalloproteinase; MS/MS, tandem mass spectrometry; P:C, proteinase:control; PCPE, procollagen C-proteinase enhancer; pNP, procollagen N-proteinase; siRNA, small interfering RNA; SMA, smooth muscle actin; TAILS, terminal amine isotopic labeling of substrates; TMT, tandem mass tag; TPP, Trans-Proteomic Pipeline; WT, wild-type

All these data completely modify the current paradigm about ADAMTS2, 3, and 14 by considerably extending their substrate repertoire.

MATERIALS AND METHODS

Antibodies

The LF-69 rabbit antiserum for the human proα1 (III) C-propeptide has been described elsewhere (14) and was kindly provided by Dr. Larry Fisher (National Institutes of Health, Bethesda, MD, USA). Mouse anti-human fibronectin N-terminal antibody was purchased from Merck Millipore (MAB1936; Darmstadt, Germany). The antibody directed against human LTBP1 was from R&D Systems (MAB388; Minneapolis, MN, USA). The goat antibody against the extracellular domain of human TGF-β RIII was from R&D Systems (AF-242-PB).

Cell lines

For inducible cell lines, human embryonic kidney (HEK) 293 cells were transfected (Novagen GeneJuice Transfection Reagent; EMD Millipore, Billerica, MA, USA) with the pcDNA 6/tetracycline repressor expression vector (Invitrogen–Life Technologies, Carlsbad, CA, USA) and selected using blasticidin (Sigma-Aldrich, St. Louis, MO, USA). Clones expressing a high level of the tetracycline repressor protein were identified by Western blotting (rabbit polyclonal #TET01; MoBiTec, Antwerpen, Belgium) and further transfected by the pcDNA4/TO expression vector (TetOn System; Invitrogen–Life Technologies) containing the complete coding sequence of ADAMTS2, ADAMTS3, or ADAMTS14 inserted in the multiple cloning site (*Not*I-*Xba*I sites for ADAMTS2 and ADAMTS14, and *Pme*I-*Pme*I sites for ADAMTS3). After selection (Zeocin, 300 μg/ml; Thermo Fisher Scientific, Waltham, MA, USA), subcloning was performed to identify clones producing ADAMTS2, ADAMTS3, or ADAMTS14 only in the presence of doxycycline (1 μM; Sigma-Aldrich).

For cell lines expressing constitutively the enzymes, HEK293 cells were transfected (Novagen GeneJuice Transfection Reagent) with the pcDNA4/TO expression vector containing the complete coding sequence of ADAMTS2, ADAMTS3, or ADAMTS14, which were inserted in the multiple cloning site (*Not*I-*Xba*I sites for ADAMTS2 and ADAMTS14, or *Pme*I-*Pme*I sites for ADAMTS3). Stably transfected cell populations were selected using Zeocin (500 μg/ml).

Recombinant proteins

Production and purification of bone morphogenetic protein (BMP)1, procollagen C-proteinase enhancer (PCPE)1, and recombinant miniprocollagen III (mini-III) were described elsewhere (15). Human plasma fibronectin was purchased from Sigma-Aldrich (#F0895). Recombinant human dickkopf-related protein (DKK)3 and TGF-β RIII were purchased from R&D Systems (#1118-DK and #242-R3, respectively). Recombinant ADAMTS2, its inactive mutant, or ADAMTS14 was produced in HEK cells and purified according to the reported procedure (16). Recombinant human TGF-β1 and TGF-β2 were from PeproTech (#100-21; PeproTech France, Neuilly-Sur-Seine, France) and Sigma-Aldrich (#T2815), respectively.

Reagents

The hyperbranched polyglycerol-aldehyde polymer was purchased from Flintbox (University of British Columbia, Vancouver,

BC, Canada). Isobaric tag for relative and absolute quantitation (iTRAQ) labels are from AB Sciex (Concord, ON, Canada). Porcine trypsin was purchased from Promega (#V511A; Madison, WI, USA). Ultrafiltration devices were purchased from Merck Millipore. All other reagents were purchased from Sigma-Aldrich. The procollagen C-proteinase–specific inhibitor (UK-383, 367) was from Sigma-Aldrich.

Secretome preparation

Dermatosparactic fibroblasts (DFs) from a patient suffering from the dermatosparactic type of Ehlers-Danlos syndrome (17) and HEK cells constitutively or conditionally (in a doxycycline-dependent manner) expressing ADAMTS2, ADAMTS3, or ADAMTS14 were cocultured in a 4:1 ratio (DF:HEK) (**Fig. 1**). The ADAMTS2 analysis is the sum of 2 experiments. In a first experiment, DFs were cocultured with HEK cells constitutively expressing the inactive (labeled iTRAQ115) or the active ADAMTS2 (labeled iTRAQ117), named TS2_A in proteome-Xchange. In this experiment, collagen synthesis was stimulated by the addition of ascorbic acid to the culture medium (25 µM). The sample before negative selection was also analyzed (named TS2_B in proteomeXchange). In a second experiment, the HEK cells expressed ADAMTS2 in a doxycycline-dependent manner (labeled iTRAQ114 and iTRAQ115, respectively, without and with doxycycline). A third condition was made by the addition of recombinant ADAMTS2 to the control secretome obtained in the absence of doxycycline (labeled iTRAQ116). There were 2 proteinase:control (P:C) ratios calculated from the latter experiment: iTRAQ115/iTRAQ114 and iTRAQ116/iTRAQ114 (named TS2_C in proteomeXchange).

The ADAMTS3 secretome was collected from HEK cells that over-express the proteinase in a doxycycline-dependent manner alone (iTRAQ115/iTRAQ114) or cocultured with DFs (iTRAQ117/iTRAQ116; named TS3_A). A second experiment was done using HEK cells alone (iTRAQ117/iTRAQ116; named TS3_B). A single experiment was performed for ADAMTS14 using the secretome of DFs cocultured with HEK cells over-expressing the proteinase in a doxycycline-dependent manner (iTRAQ117:iTRAQ116; named TS14 in proteomeXchange).

Proteinase expression was induced by adding 1 µM doxycycline 24 h before and during the 48 h of conditioned medium preparation. The secreted medium was collected after 48 h according to the reported procedure (11). Protein concentration was estimated using the optical density at 280 nm and the Bradford assay and was adjusted to 2 mg/ml. A total of 500 µg protein was processed for TAILS in each condition. When present, recombinant ADAMTS2 (23 nM) was added overnight at 37°C to the concentrated secretome.

Sample preparation for liquid chromatography-tandem mass spectrometry

As a general guideline, iTRAQ-TAILS sample preparation was done according to the reported procedure (18). For the first N-terminomics analysis of ADAMTS2 (TS2_A), the sample was fractionated on a strong cation exchange column. A linear gradient of KCl in 10 mM KH$_2$PO$_4$ was applied to elute the peptides in 10 fractions. Each fraction was injected in the mass spectrometer QStar ESI-Tof (AB Sciex) at the Protein Science Facility of the Structure Fédérale de Recherche Biosciences (Lyon, France). The sample before negative selection was also analyzed on the ESI-Q Exactive (Thermo Fisher Scientific) mass spectrometer (TS2_B). For all the other samples, peptides were injected into the ESI-Q Exactive mass spectrometer at the GIGA Proteomic Facility of the University of Liège. The mass spectrometer was coupled to a 2D-RP/RP NanoAcquity UPLC (Waters, Milford, MA, USA) for the peptide fractionation in 3 fractions. The mass spectrometry

proteomic data have been deposited to the ProteomeXchange Consortium (19) *via* the PRoteomics IDEntifications partner repository with the data set identifier PXD002354 and digital object identifier 10.6019/PXD002354.

Analysis of mass spectrometry results

In a first step, peptides were identified using Mascot (version 2.2.06; Matrix Science Inc., Boston, MA, USA) and allowing semitryptic cleavages and 2 missed cleavages/peptide. Carbamidomethyl cysteine was set as a fixed modification, and other modifications were set as variable: N-terminal acetyl, deamidation (NQ), Pyro-glu (N-term E), Pyro-Gln (N-term Q), Oxidation (M), iTRAQ (K), iTRAQ (Y) and iTRAQ (N-term). Peptide tolerance was set at 0.02 Da.

The tandem mass spectrometry (MS/MS) data were analyzed using the Trans-Proteomic Pipeline (TPP) and Proteome Discoverer software (Thermo Fisher Scientific). For the TPP analyses, the PeptideProphet and ProteinProphet software programs, embedded into TPP, used to validate protein and peptide assignment. The nontryptic model was omitted in the PeptideProphet parameters. The error rate to validate proteins or peptides was respectively set at 2 and 5%. Then, Clipper software was used to determine the upper and lower cutoffs corresponding to 3 σ calculated from the normal distribution of the log2(P:C) ratio from natural mature N termini. A Gaussian error function was used to calculate a *P* value that reflects the probability of a peptide to be a false-positive. A peptide with a P:C ratio above or below the 3 σ cutoff has ≥99.8% chance to be dependent on the studied protease (20). For data analyses with the Proteome Discoverer software, peptide assignment was validated using Percolator (embedded in the Proteome Discoverer package). Only high-confidence peptides were considered (>95% confidence). The intensity of the reporter ions was integrated using a window of 20 ppm. Clipper results were manually complemented by Proteome Discoverer data by adding missing peptides above or below the 3 σ cutoff.

Biological process analysis

The proteins showing P:C ratios above or below the cutoffs were submitted to Biological Networks Gene Ontology (BiNGO), an add-on of Cytoscape (version 2.8.2), for Gene Ontology search (21). The significance level was set at 0.005. The categories visualized are overrepresented after the Benjamini and Hochberg false discovery rate correction using the whole annotation for *Homo sapiens* in the Gene Ontology database as reference set.

Biochemical validation of the C-propeptide cleavage of type III collagen

Mouse embryonic fibroblasts (MEFs) were extracted from wild-type (WT) or ADAMTS-2 null embryos at 14.5 d postconception (dpc) and cultured under hypoxic conditions (3% O$_2$), and collagen expression was stimulated as described above. The secretome was collected according to the reported procedure (11). For Western blot analysis with the LF-69 antibody (against the C-propeptide of type III procollagen), 2.5 µg protein was loaded in each lane. Analyses of mini-III cleavage *in vitro* were all performed in 50 mM 4-(2-hydroxyethyl)-1-piperazineethanesulfonic acid (HEPES) (pH 7.5), 150 mM NaCl, and 10 mM CaCl$_2$ (HEPES buffer). ADAMTS2 or BMP1 was incubated for 16 h in the presence of 2.5 µg mini-III at 37°C in the presence or absence of 200 nM PCPE or of 250 nM UK-383,367. For N-terminal Edman sequencing (L-ProBE; Ghent University, Ghent, Belgium) of the band corresponding to the C-propeptide, proteins were electrotransferred onto a PVDF membrane and stained with Coomassie blue.
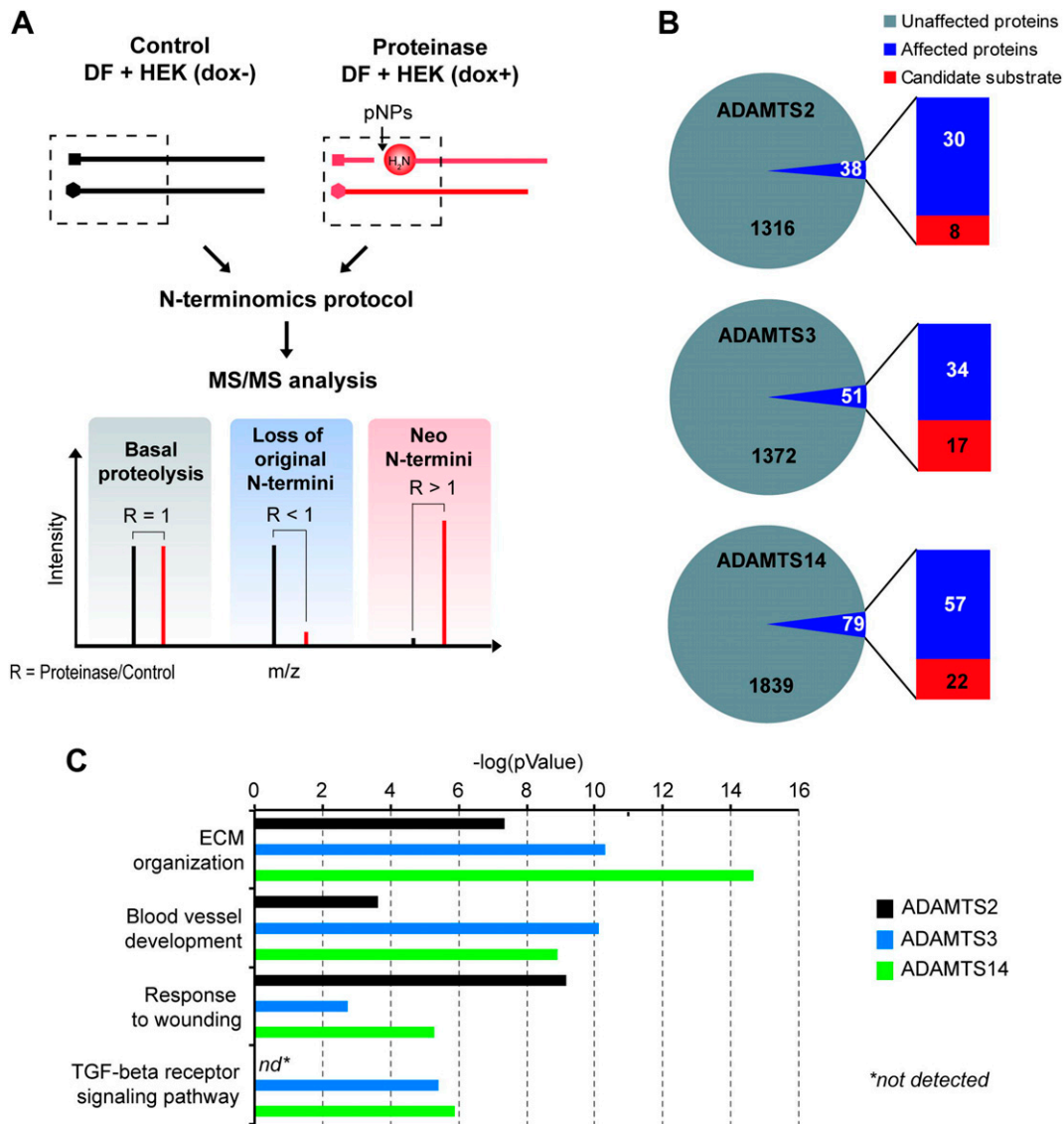
Figure 1. N-terminomics networks and biological processes related to ADAMTS2, 3, and 14. *A)* Schematic view of the N-terminomics workflow used for the analysis of the pNPs. Dashed lines show the N-terminal peptides analyzed. DFs were cocultured with HEK cells over-expressing the pNPs in a doxycycline-dependent manner (dox$^{-/+}$). *B)* Numbers of proteins observed after data analysis and affected cell surface or extracellular proteins showing at least a peptide with a ratio above or below the 3 σ cutoff of the experiment. Direct candidate substrates were defined by internal nontryptic-like peptides. *C)* Biological processes related to the pNP networks using BiNGO (21).

ADAMTS2 cleavage of fibronectin

The conditioned media of human fibroblasts were collected as described above and were then incubated with recombinant ADAMTS2 (200 nM for 16 h at 37°C) in the presence or absence of 20 mM EDTA in HEPES buffer. Western blotting was performed using the mouse anti-human fibronectin N-terminal antibody using these media or on the secretome of HEK cells expressing ADAMTS3 or 14 in a doxycycline-dependent manner. For the *in vitro* digestion, 2 μg human plasma fibronectin was incubated with recombinant ADAMTS2 (200 nM) for 16 h at 37°C in HEPES buffer. Proteins were separated using SDS-PAGE and stained with Coomassie blue. The 33 kDa cleavage product was extracted from the gel and analyzed by MS/MS. The cleavage site was determined by amino-terminal–oriented mass spectrometry of substrate (ATOMS) according to the reported procedure (22) with slight modifications developed at the GIGA Proteomic Facility: the tryptic digestion being replaced by a multienzymatic digestion based on a

mix of trypsin, chymotrypsin and GluC, and peptides being labeled with tandem mass tags [(TMTs); #90065; Life Technologies].

Analysis of DKK3 cleavage

DKK3 (2.5 μg) was incubated in the presence of ADAMTS2 (50 nM) or ADAMTS14 (100 nM), with or without 20 mM EDTA in HEPES buffer for 16 h at 37°C. Proteins were separated using SDS-PAGE and stained with Coomassie blue. The cleavage site was determined by iTRAQ-ATOMS according to the reported procedure (23). Investigation of testis morphology of WT or *Adamts2*$^{-/-}$ males was performed by hematoxylin and eosin staining of paraffin-embedded transversal sections.

Analysis of LTBP1 cleavage

LTBP1 cleavage was investigated in the secretome of HEK293 cells in the presence or absence of doxycycline for the induction

of ADAMTS expression. Proteins (2.5 µg) were separated using SDS-PAGE under nonreducing conditions to preserve the complex formed by LTBP1, latency-associated peptide (LAP), and TGF-β.

Analysis of TGF-β RIII cleavage

TGF-β RIII cleavage was assessed by Western blotting on the secretome of HEK293 cells, expressing the proteinases in a doxycycline-dependent manner, or on the secretome of human skin fibroblasts. For the *in vitro* digestion, recombinant TGF-β RIII (2.5 µg) was incubated with recombinant-purified ADAMTS2 or 14 (50 nM), in the presence or absence of 20 mM EDTA, in HEPES buffer for 16 h at 37°C. TGF-β RIII cleavage pattern was analyzed by Western blotting. For the MS/MS analysis of the cleavage products, the gel was stained with Coomassie blue, and the 50 kDa protein band observed after cleavage was extracted, digested with trypsin, and submitted to MS/MS using the ESI-Q Exactive mass spectrometer. Nontryptic peptides were also evaluated in the analysis.

Evaluation of the TGF-β response in dermal skin fibroblasts

The response to TGF-β was assessed after treatment of human normal fibroblasts with 1 ng/ml TGF-β1 or TGF-β2 for 48 h in complete medium. RNA was extracted using the RNA Isolation Kit from Roche Diagnostics (#11828665001; Meylan, France). There were 2 TGF-β target genes evaluated by RT-PCR, α-smooth muscle actin (SMA) and connective tissue growth factor (CTGF), using the RNA oligos 5′-CTAGAGACAGAGAGGAGCAGGAAA-3′ and 5′-GGCATTGCCGACCGAATGCAGAA-3′, or 5′-CCTC-GCCGTCAGGGCACTTGAA-3′ and 5′-TCCACCCGGGTTAC-CAATGACAA-3′, respectively. The RT-PCR–amplified products were quantified with GelQuant (*biochemlabsolutions.com*) and

corrected by the 28S housekeeping gene signal. Experiments were done in triplicate, errors bars are the SEMs, and the *P* values were determined using the 1-tailed unpaired Student's *t* test and GraphPad Prism (version 5.00; GraphPad Software, La Jolla, CA, USA).

Silencing of ADAMTS2 was done using a small interfering (si)RNA (siRNA) designed between the exons 13 and 14 of ADAMTS2 mRNA (NM_014244.4; National Center for Biotechnology Information; Bethesda, MD, USA) using the RNA oligos 5′-GAAGCAUGGUUACAUCAAGTT-3′ and 5′-CUU-GAUGUAACCAUGCUUCTT-3′. Cells were transfected with siRNA (20 nM), either control (scrambled, 5′-UUGCAUA-CAGGACUCGUUAUU-3′ and 5′-UAACGAGUCCUGUAUGC-AATT-3′) or specific to ADAMTS2, using the calcium phosphate precipitation procedure. After 18 h, cells were trypsinized, replated for 6 h, and treated with TGF-β1 or TGF-β2 (1 ng/ml) in complete medium. The siRNA efficiency was controlled by RT-PCR after 24 or 48 h after trypsinization using the RNA oligos 5′-GGATCTCAAACATCTTGATGTAACCA-3′ and 5′-CTACAA-GGACGCCTTCAGCCTCT-3′.

α-SMA levels were also evaluated by immunofluorescence. Cells were treated with TGF-β1 or TGF-β2 as described above. α-SMA was stained with an antibody coupled to FITC 488 (green), and nuclei were stained with DAPI (blue) (both from Sigma-Aldrich). Photographs were taken using an inverted microscope (Eclipse TI-S; Nikon, Tokyo, Japan).

Determination of cleavage site specificity

Heat maps and amino acid sequence logos, corrected by the natural abundance of amino acids in the human proteome, were generated using the iceLogo software package (24). Analyses were based on the cleavage sites determined by proteomics for the candidate substrates (**Table 1** and Supplemental Table 1).

TABLE 1. *Candidate substrates of ADAMTS2, 3, and 14 revealed by N-terminomics*

ADAMTS2		ADAMTS3		ADAMTS14	
Name	P:C (PSMs)	Name	P:C (PSMs)	Name	P:C (PSMs)
Collagen α-1(I) chain	20.1 (1)	*ADAM10*	5.7 (3)	*C3a-R*	2.5 (1)
Collagen α-2(I) chain	35.0 (1)	*ADAMTS1*	35.0 (3)	*Calsyntenin-1*	6.4 (1)
Collagen α-1(III) chain	1.7 (3)	*Clusterin*	35.0 (1)	*Collagen α-1(I) chain*	9.1 (2)
Collagen α-2(V) chain	35.0 (3)	*Collagen α-1(I) chain*	35.0 (8)	*Collagen α-2(I) chain*	35.0 (3)
Collagen α-2(VI) chain	2.0 (1)	*Collagen α-2(I) chain*	35.0 (6)	*Collagen α-1(II) chain*	4.4 (1)
Collagen α-3(VI) chain	2.0 (3)	*Collagen α-1(III) chain*	2.0 (3)	*Collagen α-1(III) chain*	2.7 (2)
Decorin	35.0 (1)	*Collagen α-1(V) chain*	4.4 (1)	*Collagen α-2(IV) chain*	3.6 (1)
DKK3	4.7 (3)	*CTGF*	7.9 (1)	*Collagen α-1(V) chain*	5.4 (4)
		Fibronectin	35.0 (1)	*Collagen α-2(V) chain*	2.7 (4)
		Fibulin-3	35.0 (1)	*Collagen α-1(XVIII) chain*	7.2 (2)
		Granulins	35.0 (3)	*Decorin*	3.7 (1)
		HLA-A	35.0 (1)	*DKK3*	7.0 (1)
		LTBP1	18.7 (2)	*Fibronectin*	4.6 (1)
		POTEJ	22.7 (3)	*Fibulin-2*	3.6 (1)
		Prosaposin	5.1 (6)	*HLA-A*	6.5 (1)
		TGF-β RIII	35.0 (2)	*IGFBP5*	5.5 (8)
		Thrombospondin-1	3.1 (2)	*LTBP1*	3.5 (1)
				LTBP2	2.5 (1)
				Lysyl oxidase	2.8 (2)
				Lysyl oxidase homolog 1	5.7 (2)
				Perlecan	6.3 (4)
				Versican core protein	8.5 (2)

Candidate substrates regarding the highest P:C ratios are shown. The highest P:C ratio of the peptides corresponding to the substrates is reported together with the number of spectra [peptide-spectrum matches (PSMs)] observed by MS/MS. The complete peptide lists for each substrate are reported in Supplemental Table 1.

RESULTS

N-terminomics analysis of ADAMTS2, 3, and 14

Investigation of the proteinase networks related to the ADAMTS2, 3, and 14

Identifications of new substrates were performed using human dermatosparactic skin fibroblasts, which lack active ADAMTS2 and only express low amounts of ADAMTS3 and 14. These cells were cocultured in a 4:1 ratio with HEK293 cells expressing or not recombinant ADAMTS2, 3, or 14. The serum-free conditioned medium of the different culture conditions was collected, and each ADAMTS-positive condition and its specific controls were labeled with different iTRAQs, pooled, and processed for TAILS analysis. In these conditions, the ratios between the intensities of the different reporter ions allow the relative quantification of peptides. Although natural N-terminal peptides and peptides corresponding to basal proteolysis lead to P:C ratios of ~1, peptides with P:C ratios significantly >1 are likely to be generated by the ADAMTS under study (Fig. 1A). In addition, the amino-terminal extremities of the protease-generated N termini (neo-N termini) correspond to the P1′ position of the cleavage sites, thereby allowing direct identification of cleavage sites. Finally, peptides with P:C ratios <1 (reflecting degradation or cell uptake of neo-N termini) are assumed to encompass the cleavage site but do not allow its precise localization. The cutoffs to discriminate neo-N termini from other N termini were determined from the normal distribution of natural N-terminal peptides, which are not expected to be modified by the proteinase. Very strict 3 σ cutoff values were used to increase the probability of identifying relevant substrates cleaved with high efficacy.

Analyses of the different culture conditions revealed the presence of 1354, 1423, and 1918 different proteins in the secretomes used for ADAMTS2, ADAMTS3, and ADAMTS14, respectively. The P:C ratios were calculated for all the identified peptides, and this indicated that 38, 51, and 79 extracellular or cell surface proteins were affected by the expression of ADAMTS2, ADAMTS3, and ADAMTS14, respectively (Fig. 1B and Supplemental Table 1). These proteins were considered to be a part of their respective protease networks (defined as the subproteome affected by the proteinase, which includes its direct substrates and secondary events linked to its expression and activity) and used to give a better insight into the biological processes related to one specific ADAMTS. BiNGO analysis (21) showed that the major processes influenced by ADAMTS2, 3, and 14 are ECM organization, blood vessel development, response to wounding, and TGF-β receptor signaling pathway (Fig. 1C). The most significant biological process was "ECM organization," with a corrected *P* value between 4.6×10^8 for ADAMTS2 and 2.2×10^{15} for ADAMTS14, principally thanks to the presence of several fibril-forming collagens and fibronectin (Fig. 1C and Supplemental Table 1). "Blood vessel development" is mostly related to ADAMTS3 and ADAMTS14, with *P* values of 7.5×10^{11} and 1.2×10^9, respectively (Fig. 1C), whereas the *P* value of ADAMTS2 was lower (2.4×10^4). ADAMTS2 and 14 are highly relevant to response to wounding (Fig. 1C). More unexpectedly, ADAMTS3 and 14 networks were related to the TGF-β receptor signaling pathway. This pathway was not identified for ADAMTS2 using BiNGO, although some of the proteins in the ADAMTS2 network (*e.g.*, LTBP1) are clearly related to this pathway according to the literature (Supplemental Table 1). Among the proteins involved in this pathway, which were affected by at least 1 of the 3 ADAMTS, were TGF-β1 and TGF-β2, the coreceptors endoglin (CD105) and TGF-β RIII, interacting and trapping molecules present in elastic fibers (LTBP1, 2, and 3; fibulins 1, 2, and 3), and other ECM macromolecules that either modulate and/or are transcriptionally regulated by the TGF-β pathway (decorin, CTGF, and collagens) (Table 1 and Supplemental Table 1).

Candidate substrates of ADAMTS2, 3, and 14

Particular attention was paid to the nontryptic-like internal peptides (no "K" or "R" in P1) having a P:C ratio >1 because these are likely to result from direct cleavage by ADAMTS, whereas tryptic peptides are more ambiguous and can also reflect changes in protein expression. This analysis yielded 8, 17, and 22 potential direct substrates for ADAMTS2, ADAMTS3, and ADAMTS14 (Table 1). Besides fibrillar collagens, ADAMTS2 was found to be likely able to process 1) the beaded filament-forming type VI collagen, outside the triple-helical domains; 2) decorin, a proteoglycan interacting with the surface of collagen fibrils; and 3) DKK3, a factor implicated in the regulation of Wnt/β-catenin and TGF-β signaling (25, 26). The potential direct substrates of ADAMTS3 were more numerous and included fibril-forming collagens, other proteins of the ECM, and proteins regulating cell behavior (apoptosis and proliferation) or lipid metabolism, such as clusterin, granulin, or prosaposin (Table 1). There were 2 cell surface receptors, human leukocyte antigen (HLA)-A and TGF-β RIII, also identified as potential substrates with high P:C ratios, suggesting that they were present as soluble forms in the conditioned medium. ADAMTS14 shares many substrates with ADAMTS2 and/or ADAMTS3, such as fibrillar collagens, fibronectin, DKK3, HLA-A, and LTBP1. Some substrates were however identified only for ADAMTS14, including 1) lysyl oxidase and lysyl oxidase like-1, 2 enzymes that crosslink collagen and elastin; 2) versican and perlecan, 2 secreted proteoglycans with multiple functions; and 3) type XVIII collagen at a site close to that involved in the release of endostatin, a potent antiangiogenic cryptic C-terminal fragment of collagen XVIII.

Although substrate identification was performed using very strict cutoff values, validation assays have to be performed. As a first step toward the validation of candidate substrates, we decided to focus on 5 of them belonging to the 2 main identified categories (ECM and signaling regulation). The potential cleavages were systematically evaluated for the 3 ADAMTS in order to get information about their substrate specificity.

Biochemical validation

Structural molecules implicated in ECM architecture and remodeling

Cleavage of the C-propeptide of type III collagen—Although ADAMTS2 can process the aminopropeptide of type III procollagen, its activity on the C-propeptide of procollagen III (CP-III) was never previously reported. Surprisingly, also, the potential cleavage site identified by N-terminomics ($G^{1221}\downarrow^{1222}D$; P:C, 1.7) is the same as for BMP1 (27). This prompted us to characterize this new potential activity of ADAMTS2 in more detail.

In order to verify the release of CP-III by ADAMTS2 (Supplemental Table 1), we used the purified enzyme and recombinant mini-III, which is composed of a short triple-helical domain, the telopeptide, and entire C-propeptide (**Fig. 2***A*) (15). ADAMTS2, but not an inactive enzyme purified in the same conditions, was able to release the CP-III (Fig. 2*B*). A similar activity was observed with ADAMTS14 (Fig. 2*C*). To further validate this *in vitro* cleavage and to confirm that this effect was not due to the copurification of a tiny amount of BMP1, the assay was also performed in the presence of a BMP1 synthetic inhibitor and/or in the presence of a specific enhancer of BMP1 activity on procollagen (PCPE) (29). ADAMTS2 cleaved the C-propeptide of type III collagen to the same extent regardless of the presence of the inhibitor or the enhancer (Fig. 2*D*). These results demonstrate that the C-propeptide of type III collagen is directly cleaved by ADAMTS2.

The ADAMTS2 cleavage site within mini-III was determined by N-terminal Edman sequencing and yielded the following cleavage site: $G-F-A-P^{1218}\downarrow^{1219}Y-Y-G-D$ (Fig. 2*A*). The Proline in the P1 position was also previously found in the N-propeptide cleavage site (1), but it is located 3 residues N terminal to the site identified by N-terminomics. The discrepancy between the 2 approaches could be related to the presence of BMP1 in the conditioned culture medium, the activity of which is possibly increased when there is prior cleavage by ADAMTS.

To explore the biological significance of this cleavage, type III collagen processing was assessed in MEFs from 6 different embryos (3 WT and 3 $Adamts2^{-/-}$) at 14.5 dpc. An antibody specific to the C-propeptide (LF-69) was used and showed a reduction in the amount of "free" C-propeptide together with the accumulation of pC forms when ADAMTS2 was absent (Fig. 2*E*).

Cleavage of cellular and plasma fibronectin—Fibronectin is another important component of the ECM. It is also abundant in plasma under a form lacking type III-A and type III-B domains (Fig. 2*F*). TAILS analyses indicate a possible cleavage site in the N-terminal domain (P:C, 0.12; Supplemental Table 1). Validation studies were performed by Western blotting using an antibody specific to the 30 kDa N-terminal domain (Fig. 2*G*). Media conditioned by normal human skin fibroblasts contained a fragment migrating ~33 kDa by SDS-PAGE. In contrast, accumulation of full-length fibronectin and absence of this 33 kDa product were observed in the medium of DFs (Fig. 2*G*). When recombinant-purified ADAMTS2 was added in vitro into the DF-conditioned medium, the 33 kDa product was also generated at the expense of the full-length fibronectin (Fig. 2*G*), and this processing was abolished in the presence of EDTA. Noteworthy, the release of the 33 kDa fibronectin fragment was also specifically observed in the conditioned medium of HEK293 cells expressing ADAMTS3 or ADAMTS14 compared to nontransfected cells (Fig. 2*H*), suggesting that this activity is shared by all 3 enzymes.

In a second step, plasma fibronectin was also incubated *in vitro* with recombinant-purified ADAMTS2, resulting in a similar product of ~33 kDa (Fig. 2*I*). The full-length fibronectin and its C-terminal fragment after cleavage by ADAMTS cannot be easily separated using SDS-PAGE, making classic (Edman) N-terminal sequencing difficult to implement. Therefore, the 33 kDa fragment from plasma fibronectin was analyzed by mass spectrometry. In agreement with the specificity of the antibody used in Western blotting, the peptides observed by mass spectrometry cover the N-terminal assembly domain of fibronectin. The precise cleavage site was then determined using a new approach called ATOMS (22, 23) coupled to TMT labeling and to a multienzymatic digestion. The 5 peptides with the highest P:C ratios resulted from a unique and unambiguous cleavage site: $V-R-A-A^{292}\downarrow^{293}V-Y-Q-P$ (Fig. 2*J*). This cleavage site was not seen using a classic tryptic digestion such as in N-terminomics. This is likely due to the size of the tryptic peptide resulting from this cleavage site, which is too long (32 amino acids, 3.6 kDa) to be properly assigned by MS/MS.

Cell signaling molecules

Cleavage of DKK3 by ADAMTS2 and 14—DKK3 is a member of the DKK family, which comprises 4 members characterized by 2 conserved cysteine-rich domains (Fig. 3*A*). N-terminomics analyses indicated cleavage of DKK3 by ADAMTS2 and ADAMTS14 (Supplemental Table 1), a result that was confirmed in vitro using recombinant human DKK3 in the presence of recombinant ADAMTS2 or 14 (Fig. 3*B*). DKK3 is a highly glycosylated molecule migrating at 75–80 kDa by SDS-PAGE despite a predicted mass of 37.5 kDa. In the presence of ADAMTS2 or 14, the intensity of the corresponding band decreased, whereas 3 cleavage products migrating at 38, 55, and 70 kDa were observed (Fig. 3*B*). According to the N-terminomics analyses, DKK3 was cleaved at positions $^{126}M\downarrow V^{127}$, $^{128}F\downarrow S^{129}$, and $^{130}E\downarrow T^{131}$. To determine the precise cleavage site of ADAMTS2 within DKK3, we used iTRAQ-ATOMS on recombinant proteins in vitro, which led to the identification of a single cleavage site at position $^{126}M\downarrow V^{127}$ (Fig. 3*A*). This suggests the existence of sequential secondary processing by other proteinases after initial ADAMTS2 cleavage or that the cleavage site is perhaps less strictly defined in conditions encountered in cell culture. The generation of 3 degradation products of DKK3 (38, 55, and 70 kDa) by ADAMTS2 or ADAMTS14 suggests the presence of at least 2 cleavage sites. This second site might be the $^{252}I\downarrow T^{253}$ identified for ADAMTS14 during the N-TAILS analysis. The reason why this site was not identified by iTRAQ-ATOMS on recombinant proteins was not investigated further.

DKK3 has been shown to be implicated in seminiferous tubule development (30). Therefore, the histology of testes from adult WT or $Adamts2^{-/-}$ mice was examined by
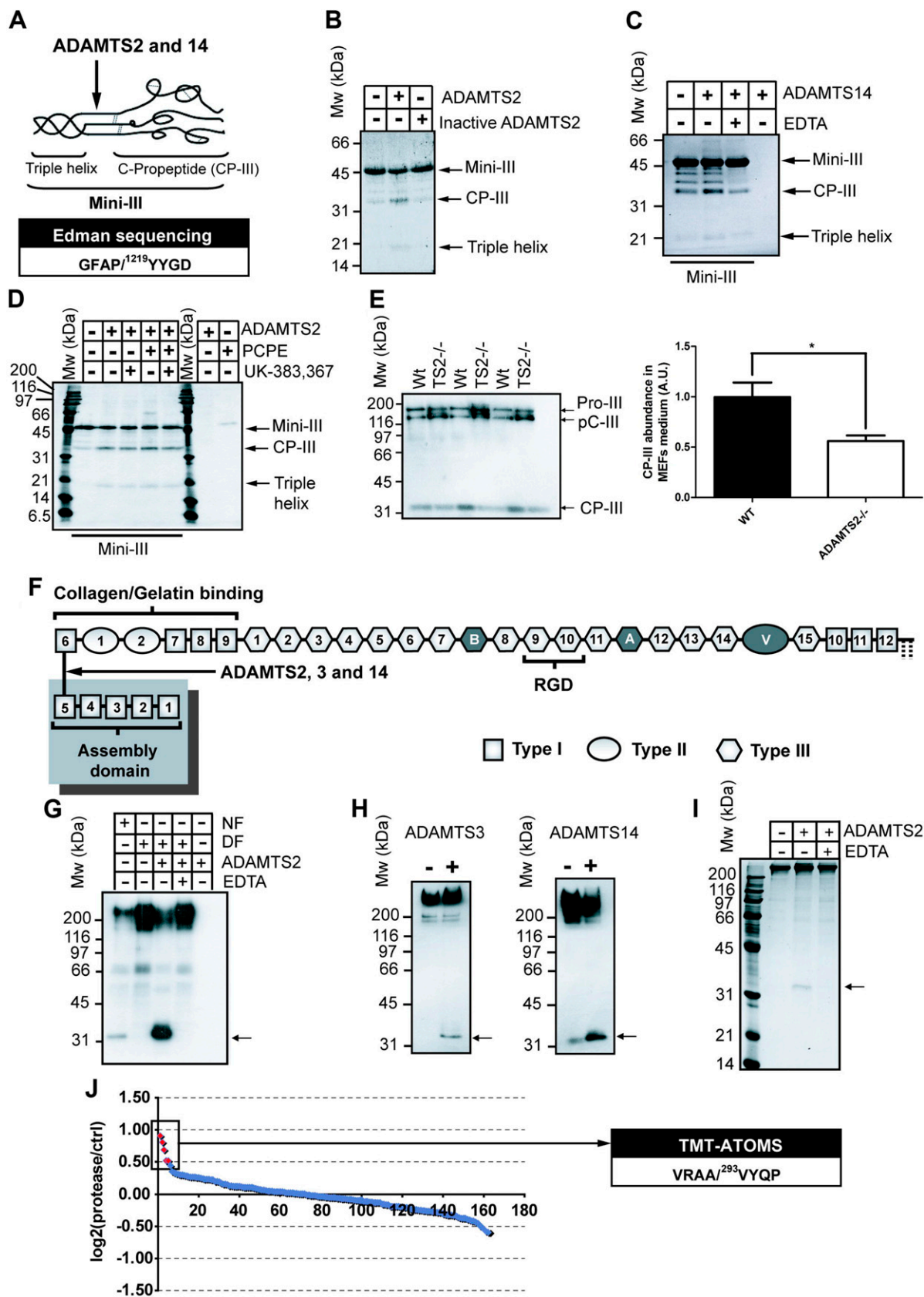
Figure 2. Novel proteolytic events of the pNPs related to structural molecules of the ECM: CP-III and fibronectin. *A*) Schematic view of the recombinant procollagen III model substrate (mini- III). The cleavage site determined by N-terminal Edman sequencing is reported below. *B* and *C*) SDS-PAGE (10% acrylamide, reducing conditions) stained with Coomassie blue shows the *in vitro* digestion of recombinant mini-III (850 nM) by recombinant-purified ADAMTS2 (50 nM) or its inactive mutant (*B*) or

(continued on next page)

hematoxylin and eosin staining. The seminiferous tubules were altered in *Adamts2*$^{-/-}$ mice with an increase in lumen space and a reduction in thickness of the tubules (Fig. 3*C*), which complemented previous findings showing a decrease of mature sperm in *Adamts2*$^{-/-}$ testes (3). ADAMTS2 cleaves DKK3 upstream of the 2 conserved cysteine-rich domains known to be responsible for the inhibition of the Wnt pathway. Therefore, DKK3 processing by ADAMTS could activate, rather than abolish, its inhibitory function on the Wnt pathways. Because DKK3 is involved in seminiferous tubule development (30), it is tempting to speculate that the infertility of *Adamts2*$^{-/-}$ male mice could be related to dysregulation of DKK3 function in testis.

LTBP1 processing—LTBP1 sequesters pro-TGF-β within the ECM to allow its rapid release when needed. The association of LTBP1 with pro-TGF-β by disulfide links is known as the large latent complex (LLC) (Fig. 4*A*). N-terminomics analyses revealed the cleavage of LTBP1 by ADAMTS3 at ^{315}P↓A^{316} and ^{775}P↓A^{776} positions (Fig. 4*A*). LTBP1 processing by ADAMTS3 was first confirmed by Western blotting in the medium of HEK293 cells expressing the proteinase (Fig. 4*B*). In the absence of ADAMTS3, 2 bands of 250 and 185 kDa were observed, which corresponded, respectively, to the LLC (LTBP1 associated with pro-TGF-β1) and to LTBP1 alone (Fig. 4*B*). When ADAMTS3 was expressed, the relative intensity of LLC decreased, whereas a cleavage product of 150 kDa, corresponding to the expected size after cleavage of LTBP1 at the ^{315}P↓A^{316} site, was markedly increased (Fig. 4*A*, *B*). No band of 104 kDa that would have resulted from the cleavage at the ^{775}P↓A^{776} site could be observed.

Proteomic analyses identified LTBP1 cleavage by ADAMTS14 at the ^{36}P↓G^{37} position (Fig. 4*A* and Supplemental Table 1). This should generate a cleavage product differing by only 1.5 kDa from the uncleaved LTBP1, which does not allow their discrimination by SDS-PAGE. When ADAMTS14 was expressed in HEK293 cells, LLC abundance decreased, whereas the band corresponding to LTBP1 alone increased (Fig. 4*C*), leading to a different electrophoretic pattern from that obtained with ADAMTS3. Because dissociation of LAP/TGF-β from LTBP1 should not result from a cleavage at the ^{36}P↓G^{37} site, it must be caused by a cleavage within the LAP domain (see Fig. 4*A*).

This hypothesis is further supported by the existence of a cleavage site in the LAP domain of TGF-β1, as suggested by the proteomic analysis (P:C, 0.28; Supplemental Table 1).

For ADAMTS2, a well-defined band corresponding to a degradation/maturation product was never detected. However, a slight decrease of the LLC intensity was consistently observed, suggesting that a cleavage that modifies or destroys the epitope recognized by the LTBP1 antibody may occur (Fig. 4*D*). In summary, it seems that whereas all the studied ADAMTSs are susceptible to cleave the LLC, there are significant differences in their cleavage specificity.

Cleavage of TGF-β RIII by ADAMTS2, 3, and 14—N-terminomics analyses identified a cleavage of TGF-β RIII (β-glycan) by ADAMTS3 between the endoglin-like and the *zona pellucida* domains (Fig. 5*A*) at the ^{383}P↓^{384} site. TGF-β RIII cleavage was first assessed by Western blotting in the conditioned medium of inducible HEK cells. Because TGF-β RIII is a transmembrane receptor, only shed fragments could be identified in these conditions. The same pattern was observed in the presence of the 3 ADAMTS, with an increased abundance of 2 cleavage products of 50 and 60 kDa (Fig. 5*B*). To get further insight into the physiological relevance of this cleavage, Western blots were performed on the conditioned medium of normal and DFs. Although some intact shed ectodomain of TGF-β RIII could be seen with DFs, only the cleaved forms were present in the media of normal fibroblasts (Fig. 5*C*).

To assess the direct cleavage of TGF-β RIII, *in vitro* assays were performed using purified recombinant TGF-β RIII and ADAMTS2 or ADAMTS14. A band migrating ~120 kDa (Fig. 5*D*), accompanied by a higher molecular mass smear typical of proteoglycans, was observed in the presence of EDTA (Fig. 5*D*). In the presence of active ADAMTS2 or ADAMTS14, however, the intact soluble TGF-β RIII disappeared, and a single cleavage product was observed ~50 kDa (Fig. 5*D*). No other cleavage product was seen using either Western blotting (Fig. 5*D*) or Coomassie blue staining. The 60 kDa band observed in Fig. 5*B* could therefore be due to glycosylation or to an additional cleavage, occurring only in a cellular context, by ADAMTS2, 3, or 14 or other proteases. The 50 kDa band was analyzed by MS/MS and shown to correspond to the N-terminal endoglin-like domain resulting from a cleavage at the

ADAMTS14 (200 nM) with or without EDTA (20 mM, *C*). Mw, molecular weight. *D*) Digestion of mini-III by ADAMTS2 (50 nM) in the presence or absence of PCPE-1 (200 nM) with or without the specific BMP1 inhibitor (UK-383,367; 250 nM) (28). *E*) Type III collagen processing in the conditioned medium of MEFs extracted from 6 different embryos (WT or *Adamts2*$^{-/-}$) at 14.5 dpc. The Western blot was performed using an antibody specific to the C-propeptide of type III collagen (LF-69, left). Estimation of C-propeptide release in the MEF secretome (WT or *Adamts2*$^{-/-}$) is shown. Error bars represent ±SEM. *P = 0.0235, determined using the 1-tailed unpaired Student's *t* test. *F*) Schematic view of the fibronectin molecule. Type I, II, and III fibronectin domains are represented by gray squares, circles, or hexagons, respectively. The alternatively spliced extra fibronectin type III domains (*A*, *B*) and the variable region are shown in dark gray. The binding site to the integrins [encompassing the tripeptide Arg-Gly-Asp (RGD) motif] is underlined. The ADAMTS2, 3, and 14 cleavage site is indicated with an arrow. *G*) Immunoblots of the secretome of human normal fibroblasts (NF) or DFs using an antibody specific to the N-terminal (30 kDa) part of human fibronectin. Recombinant-purified ADAMTS2 (75 nM) was added *in vitro* to the secretome of DFs with or without EDTA (20 mM). *H*) Western blots of the secretome of HEK cells expressing ADAMTS3 or 14 in a doxycycline-dependent manner, using the anti-N-terminal domain of fibronectin antibody. *I*) *In vitro* digestion of human plasma fibronectin by recombinant ADAMTS2 shown by SDS-PAGE (12.5% acrylamide, reducing conditions) stained with Coomassie blue. The cleavage product of ~33 kDa corresponding to the N-terminal domain was identified by MS/MS using the protein band extracted from the gel. *J*) Fibronectin cleavage site in the presence of ADAMTS2 was determined using TMT-ATOMS. The samples were digested with a mix of proteases before analysis. A total of 163 peptides labeled with TMTs at their N termini were observed, most of them having TMT ratios of ~1 and derived from partial degradation of the commercial fibronectin preparation. The P:C ratios of those peptides are shown with a graphic representation of log2[protease/control (ctrl)]. The 5 peptides with the highest P:C ratio (red dots) originate from the same cleavage site and unambiguously define the preferential ADAMTS2 cleavage site within fibronectin. This cleavage site is reported on the right.
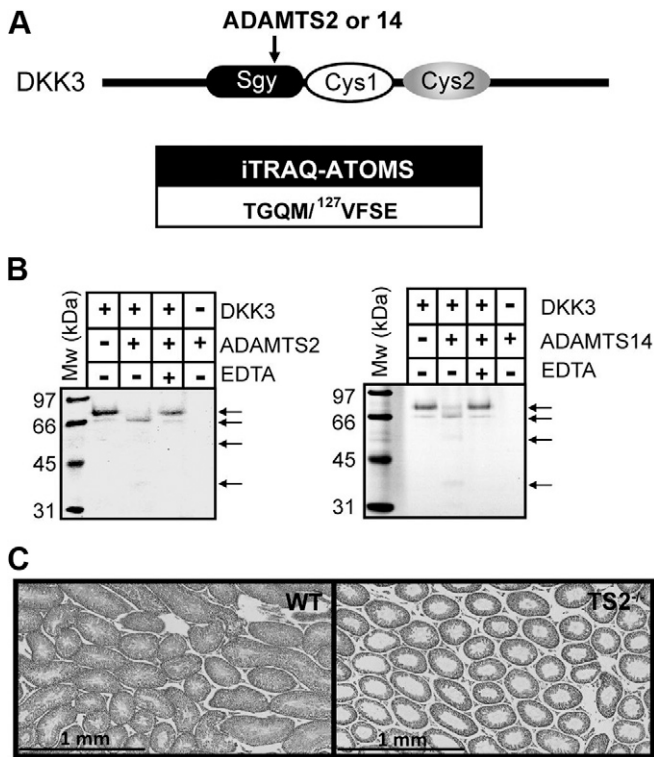
Figure 3. ADAMTS2 or 14 cleavage of DKK3 and potential implication in testis development. *A*) Schematic view shows the domain composition of DKK3. One of the cleavage sites observed by N-terminomics in complex media was confirmed by iTRAQ-ATOMS using recombinant proteins *in vitro*. The cleavage site determined by iTRAQ-ATOMS is reported below [P:C, 11.96; peptide-spectrum matches (PSMs), 8]. *B*) *In vitro* digestion of recombinant human DKK3 by recombinant-purified ADAMTS2 (left) or ADAMTS14 (right). Proteins were visualized by SDS-PAGE (10% acrylamide, reducing conditions) stained with Coomassie blue. Mw, molecular weight. *C*) Hematoxylin and eosin staining of paraffin-embedded sections of testes of 8-wk-old WT or $Adamts2^{-/-}$ (TS2$^{-/-}$) mice ($n = 2$).

^{383}P↓A^{384} cleavage identified by N-terminomics for ADAMTS3 (Fig. 5*E*).

Implication of ADAMTS2 in the TGF-β response of skin fibroblasts Many substrates identified in this study indicated that ADAMTS2, 3, and 14 play a major role in the regulation of TGF-β signaling. Using ADAMTS2 as a model proteinase, the response of human skin fibroblasts to TGF-β1 or -β2 was evaluated by RT-PCR (Fig. 6*A*) using α-SMA and CTGF as reporter genes. The specific contribution of ADAMTS2 was assessed using an siRNA directed against this protease (Fig. 6*A*). After treatment with TGF-β1 or TGF-β2, the induction of α-SMA or CTGF was attenuated in fibroblasts deficient in ADAMTS2 (Fig. 6*B*, *C*). Similar data were obtained when the response of normal and DFs was compared (data not shown). This reduction of TGF-β response was slightly more potent in the presence of TGF-β2 compared to TGF-β1 treatment (Fig. 6*B*, *C*), suggesting a contribution from TGF-β RIII, which is known to have a higher affinity for TGF-β2. The response of human fibroblasts to TGF-β in the absence of ADAMTS2 was also verified by immunofluorescence (Fig. 6*D*). When fibroblasts were treated with TGF-β1 or 2, a clear induction of α-SMA was seen. In agreement with the RT-PCR data, after TGF-β treatment, the α-SMA level was reduced when ADAMTS2 is silenced, confirming the specific contribution of ADAMTS2 to the TGF-β response.

Cleavage site specificity of ADAMTS2, 3, and 14

Cleavage site specificities were analyzed based on cleavage events related to the candidate substrates (Table 1 and Supplemental Table 1) complemented with the cleavage sites determined by Edman or ATOMS. To take into account the contribution of the particular nature of fibrillar collagens (rich in Glycine and Proline), the analysis was performed with and without the cleavage sites of type I collagen (α-1 and α-2 chains) (**Fig. 7**). When collagen I was excluded, the cleavage sites of all 3 ADAMTS shared a common and specific enrichment in small nonpolar or slightly hydrophobic amino acids (G, P, A, M, F, and V) in the P1 and P1′ positions (Fig. 7, right panels). According to this analysis, the preferential cleavage site for the pNPs is P/A↓G/V. Including collagen I cleavage sites in the analysis does not modify the deduced ADAMTS3 specificity but affects slightly the consensus cleavage site for ADAMTS2 and 14, notably by increasing the contribution of the Glycine residue in P1′ (Fig. 7).

DISCUSSION

Recent data indicated that ADAMTS2, 3, and 14 could be involved in biological functions that are not related to collagen processing (31) and may thus have other physiological substrates (32). This hypothesis was evaluated using an N-terminomics approach that allows the identification of new substrates in complex samples, as already demonstrated with several metalloproteinases such as MMPs and meprins (12, 13). Using this approach, we identified several new extracellular and cell surface potential substrates of ADAMTS2, 3, and 14, of which some were validated by Western blotting, N-terminal sequencing, and/or mass spectrometry analysis. In this work, the proteins identified by N-terminomics on cell cultures constitute a subproteome (or protease network) related to the expression of ADAMTS2, 3, or 14. Under these experimental conditions, the protease network includes the primary direct substrates of the studied enzymes. It contains also proteins that are indirectly affected as a result of activation or inhibition of other actors such as other proteinases, inhibitors of proteinases, or cytokines. As a whole, the protease networks determined here in well-characterized models are therefore fully relevant to the biological functions of ADAMTS2, 3, or 14. Altogether, the N-terminomics and validation data have led to the identification of preferential cleavage sites. For the 3 ADAMTSs, the P1 and P1′ positions were enriched in nonpolar or slightly hydrophobic amino acids (mainly G, P, A, M, F, and V), a very unique specificity that strongly differs from that reported for BMP1 (D in P1′), MMP2 and 9 (L in P1′), or ADAMTS1 or 4 (E in P1). It is worth mentioning that the previously identified cleavage site allowing the release of the aminopropeptide of type I, II, and III procollagens (A/P↓Q) could not be identified here because the
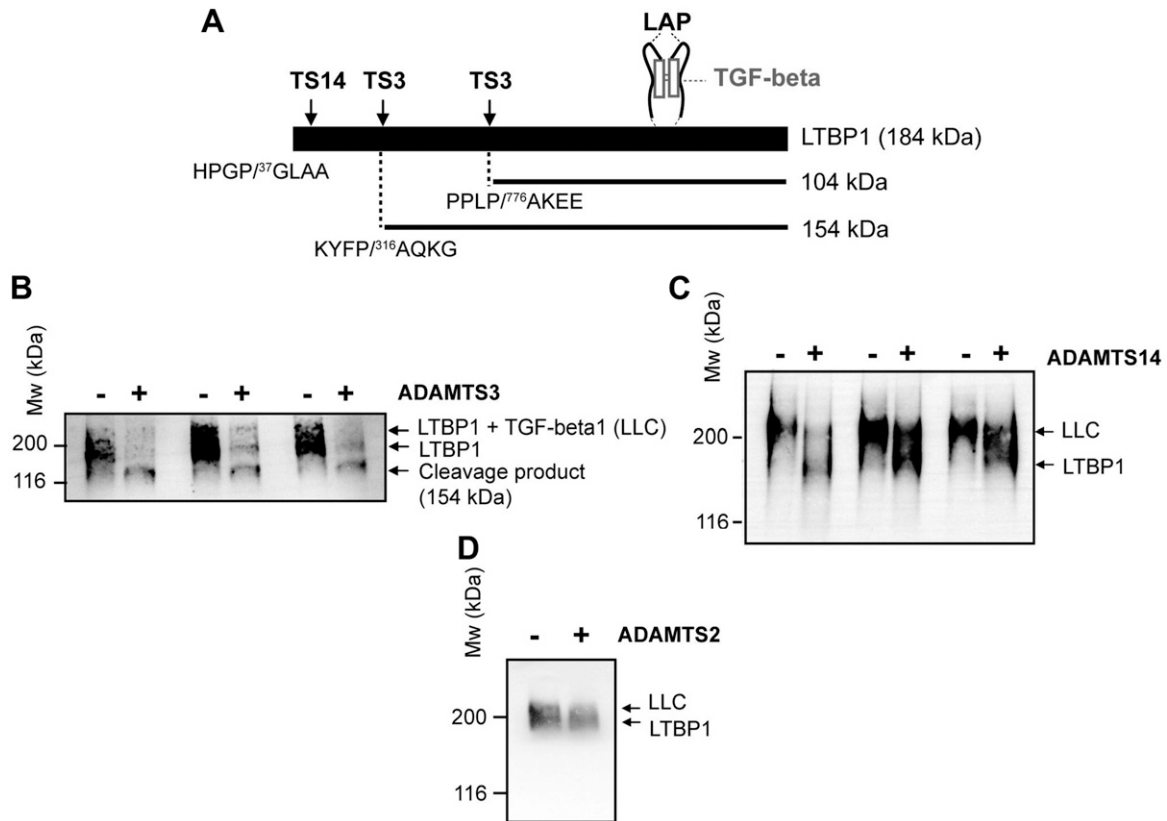
Figure 4. LTBP1 cleavage by the pNPs. *A*) Schematic view of the LLC composed of LTBP1 associated with pro-TGF-β1, the latter being secreted as a noncovalent complex between TGF-β and the LAP. ADAMTS3 and 14 cleavage sites within human LTBP1, observed by N-terminomics, are shown by black arrows. Cleavage site sequences are reported below. *B–D*) Western blots using an anti-human LTBP1 antibody on the secretome of HEK cells expressing ADAMTS3 (*B*), ADAMTS14 (*C*), or ADAMTS2 (*D*) in a doxycycline-dependent manner. Proteins were separated by SDS-PAGE (7.5% acrylamide). Experiments were performed under nonreducing conditions to see the LLC. Mw, molecular weight.

proteins in the secretome were not treated to remove the blocked terminal pyroglutamate. The previously published "P↓A" processing of α-1 type V procollagen was however identified and confirmed the reliability of our experimental procedure (Supplemental Table 1). Similarly, several "A↓A" sites were identified, which fully correspond to the newly identified cleavage of VEGF-C by ADAMTS3 (10). Several different cleavage sites were also identified in the triple-helical domain of type I collagens (Supplemental Table 1). This was not anticipated but is not surprising based on the identification here of the preference of these ADAMTSs for proline- and glycine-rich sequences and knowing that the high expression of collagens by fibroblasts in culture leads to the secretion of a significant percentage of abnormally folded collagen molecules, which increases the possibility to identify true, although rare, cleaved sequences.

The similarity between the preferential cleavage sites for ADAMTS2, 3, and 14 certainly explains why they share several common substrates (such as fibronectin or TGF-β RIII). However, it is clear that substrate specificity is also governed by structural interactions between the substrate and the protease ancillary domains that are less conserved than the catalytic domain. This is probably the case for LTBP1 because the 3 studied ADAMTSs did not generate the same products.

The cleavage of the N-terminal domain of fibronectin by ADAMTS2 was confirmed using normal and DFs.

Interestingly, fibronectin has been reported to be implicated in platelet thrombus formation and diseases associated with thrombosis (33), and this could be correlated to previous results showing that ADAMTS2 is potentially involved in pediatric stroke and that its expression is increased in atherosclerotic plaques causing acute myocardial infarction (9). Fibronectin is also known to be involved in inflammation by recruiting and activating leukocytes, notably through its 29 kDa N-terminal fragment that can be released by thrombin (34). Moreover, the ADAMTS2 proteinase network shows other links with proteins involved in inflammation (see Supplemental Table 1: collagen α-2(VI) and α-3(VI) chains, IL-8, macrophage migration inhibitory factor, or the complement C1s subcomponent), which supports the role of ADAMTS2 in the immune system (4).

This study reports the unexpected cleavage of cell signaling molecules such as DKK3, which is implicated in prostate morphogenesis (26, 35) and testis development (30) probably through the regulation of TGF-β or Wnt/β-catenin signaling. Investigation of testis morphology in *Adamts2*$^{-/-}$ male mice shows the alteration of the seminiferous tubules leading to the interesting hypothesis that processing of DKK3 by ADAMTS2 could play a role during testis development. However, the exact mechanism needs to be studied more precisely.
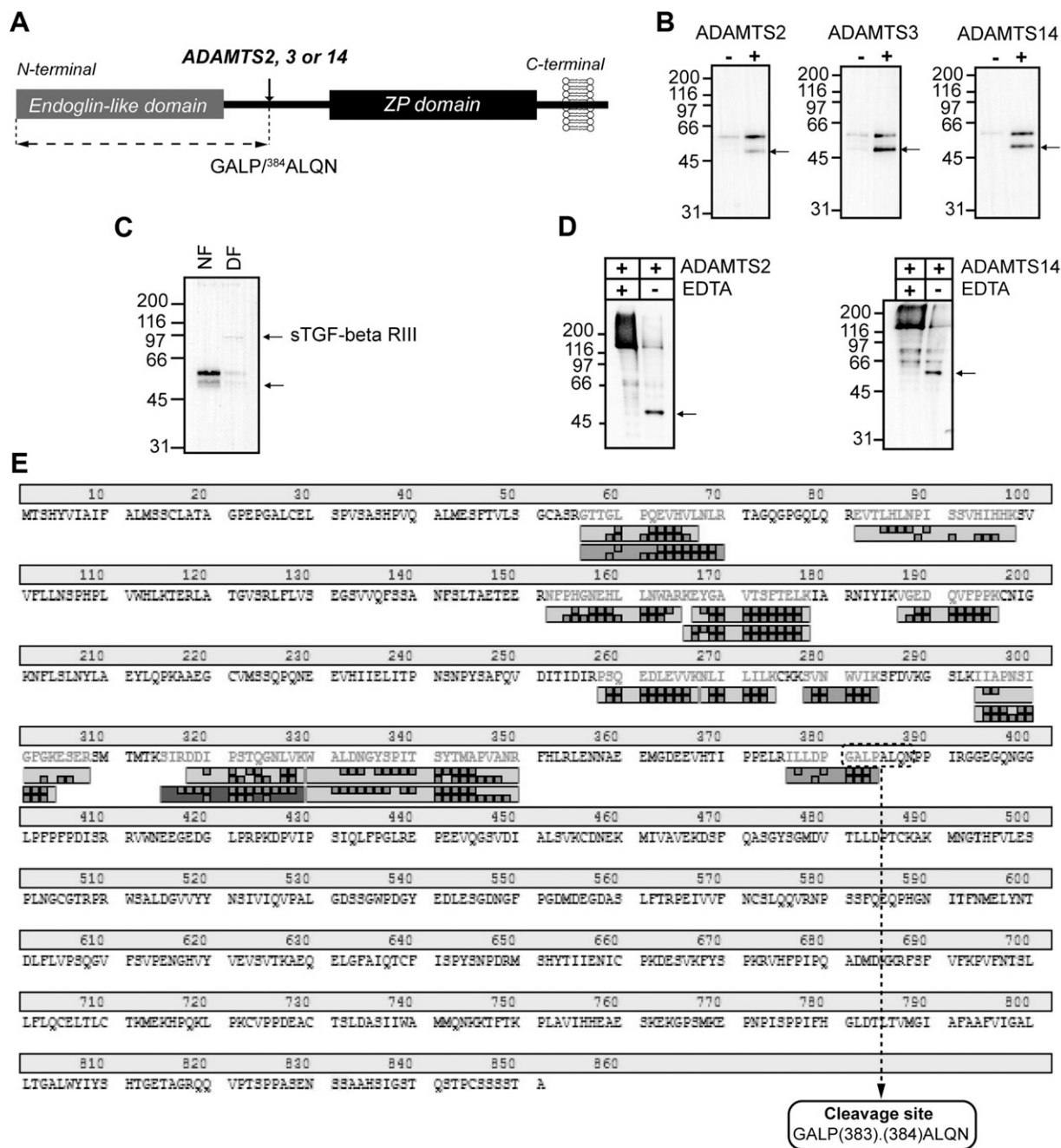
Figure 5. TGF-β RIII cleavage by ADAMTS2, 3, and 14. A) Schematic view of TGF-β RIII shows the cleavage site observed by N-terminomics and confirmed by MS/MS identification of the cleavage product in gel (Supplemental Table 1; see below). B) Western blot for TGF-β RIII in the medium of HEK cells over-expressing ADAMTS2, 3, or 14. The direct cleavage product is indicated by arrows. C) Western blot analysis of TGF-β RIII present in the medium of human normal fibroblasts (NF) or DFs. The shed form (sTGF-β RIII) is indicated by an arrow. D) Western blot shows the digestion of recombinant-purified TGF-β RIII (2.5 μg) by recombinant ADAMTS2 (left) or 14 (right) in vitro. The only cleavage product, observed using Coomassie staining and identified by MS/MS, is the endoglin-like domain (arrow). E) Liquid chromatography-tandem mass spectrometry identification of the 50 kDa TGF-β RIII product generated by ADAMTS2 cleavage. Semitrypsin digestion was set as parameter for the identification of the peptide sequences. The cleavage product ends at the cleavage site determined by N-TAILS.

Analyses of the proteinase networks reveal a strong link between pNPs and TGF-β signaling. This is in line with previous data showing that 1) mutations affecting ADAMTS10, ADAMTS17, ADAMTSL2, or ADAMTSL4 proteins are involved in genetic diseases related to elastic fibers and TGF-β (36, 37); 2) the absence of ADAMTS2 reduces liver fibrosis (38); and 3) ADAMTS enzymes are characterized by the presence of one or several domains similar to the "thrombospondin type I repeat" domain known to activate pro-TGF-β1 (39, 40).

This study reports new mechanisms by which ADAMTS2, 3, and 14 can collectively modulate TGF-β signaling, through the cleavage of LTBP1, TGF-β RIII, and probably, pro-TGF-β. The direct cleavage of LTBP1 was
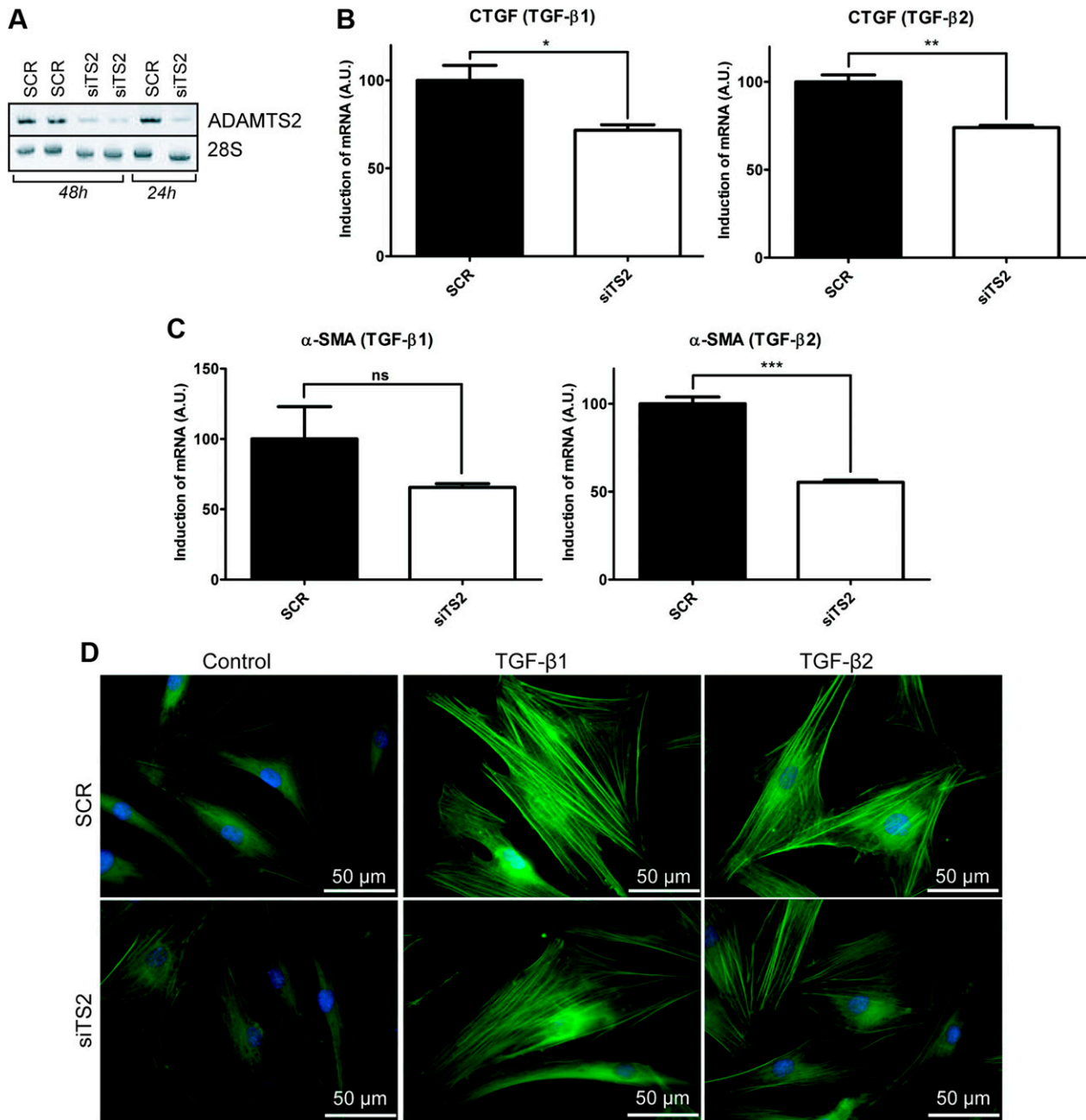
Figure 6. Biological implication of ADAMTS2 in TGF-β signaling in human fibroblasts. *A*) Assessment of ADAMTS2 silencing by RT-PCR after 24 or 48 h. Human normal dermal fibroblasts were transfected with a scrambled siRNA or an siRNA directed against ADAMTS2. *B* and *C*) Investigation of TGF-β response in human fibroblasts by RT-PCR using 2 TGF-β target genes: CTGF (*B*) and α-SMA (*C*). Human normal fibroblasts were transfected with a scrambled (SCR) or a specific siRNA (siTS2) for ADAMTS2 and were treated with 1 ng/ml TGF-β1 (left panel) or TGF-β2 (right panel) for 48 h. A.U., arbitrary units. Experiments were done in triplicate. Error bars are ±SEM. ns, 0.1046; *P = 0.0178, **P = 0.0017, and ***P = 0.0002, determined using the 1-tailed unpaired t test. *D*) Investigation of α-SMA level in human fibroblasts by immunofluorescence (FITC, green). Nuclei were stained with DAPI. Cells were treated as described above.

clearly demonstrated for ADAMTS3, which induces the release of TGF-β immobilized in the ECM. In the case of ADAMTS2 or 14, a specific cleavage site in LTBP1 inducing such release could not be identified. However, Western blot analyses showed that the LLC (formed by LTBP1, LAP, and TGF-β) is less abundant in the presence of ADAMTS2 or ADAMTS14. This suggests either that LTBP1 is cleaved at a site that is different from the ADAMTS3 cleavage site and could not be identified in our experimental conditions

or that cleavage occurs in the LAP or in TGF-β itself (see Fig. 4*A*). In favor of the latter hypothesis, N-terminomics data showed that ADAMTS14 cleaves the pro-TGF-β molecule between the LAP domain and C-terminal sequence corresponding to mature TGF-β (Supplemental Table 1).

The cell surface receptor TGF-β RIII is known to act as a coreceptor for TGF-β signaling and notably for TGF-β2 (41, 42). TGF-β RIII can also be shed from the cell surface to release a soluble form that acts as an inhibitor of TGF-β

Figure 7. Analysis of the cleavage site specificities of ADAMTS2, 3, and 14. Data are shown for ADAMTS2 (*A*), ADAMTS3 (*B*), and ADAMTS14 (*C*) with (left) or without (right) type I collagen cleavages. The analyses were based on 18, 31, and 45 cleavage events (left) or 8, 26, and 23 cleavage events (right) respectively for ADAMTS2, ADAMTS3, and ADAMTS14. Cleavage sites determined by N-terminal Edman sequencing or ATOMS were used to complement the proteomic analysis. Amino acid sequence logos were generated using the iceLogo software package (24). The height of 1 amino acid reflects its frequency; the color represents its physicochemical properties.
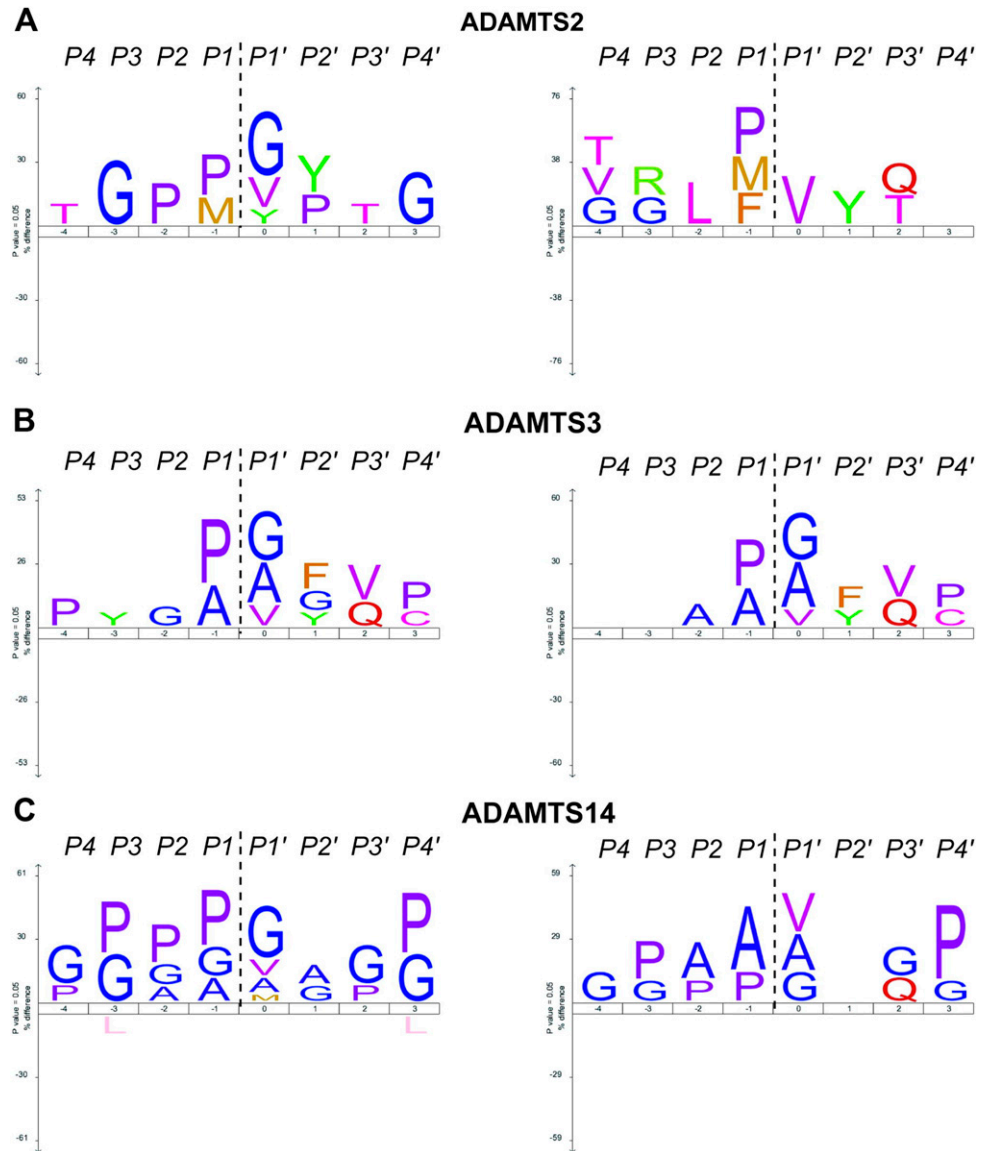
signaling (43–45). Cleavage of the soluble TGF-β RIII within the nonstructured linker between the N-terminal endoglin-like domain and the *zona pellucida* domain hampers its ability to inhibit TGF-β signaling because both domains are required for the recognition of the growth factors of the TGF-β superfamily (23, 45, 46). Therefore, cleavage of the soluble TGF-β RIII by the pNPs within the nonstructured linker will also contribute to increase TGF-β availability.

Cleavage of LTBP1 and soluble TGF-β RIII by the pNPs should both lead to activation of TGF-β signaling. This hypothesis was evaluated in human skin fibroblasts using ADAMTS2 as a model. Our data clearly show that the response to TGF-β1 and -β2 is down-regulated in the absence of endogenous ADAMTS2. Additional characterizations will be required to identify more precisely the relative contribution of the different cleavages (LTBP1, pro-TGF-β, and/or TGF-β RIII). Because ADAMTS2 expression is induced by TGF-β (47), its role in TGF-β signaling reported here constitutes a positive feedback loop that could be involved in processes such as fibrosis or wound healing (48, 49). We have reported that tetrachloride-induced liver fibrosis is reduced in *Adamts2*$^{-/-}$ mice, implying the involvement of ADAMTS2 in fibrosis (38). This function was initially assumed to be due only to alterations in amino procollagen processing, but the involvement of ADAMTS2 in the cell response to TGF-β reported here could be an important additional mechanism.

In conclusion, this original analysis of the substrate repertoire of ADAMTS2, 3, and 14 shed a new light on the dogmatic idea that ADAMTS2, 3, and 14 are only involved in amino procollagen processing. Because they are able to cleave many ECM macromolecules but also proteins directly regulating cell phenotype such as factors involved in Wnt and TGF-β pathways, they should now be considered as multilevel regulators of ECM deposition and remodeling. ⏴ᴊ⏵

REFERENCES

1. Bekhouche, M., and Colige, A. (2015) The procollagen N-proteinases ADAMTS2, 3 and 14 in pathophysiology. *Matrix Biol.* **44–46**, 46–53

2. Nusgens, B. V., Verellen-Dumoulin, C., Hermanns-Lê, T., De Paepe, A., Nuytinck, L., Piérard, G. E., and Lapière, C. M. (1992) Evidence for a relationship between Ehlers-Danlos type VII C in humans and bovine dermatosparaxis. *Nat. Genet.* **1**, 214–217

3. Li, S. W., Arita, M., Fertala, A., Bao, Y., Kopen, G. C., Långsjö, T. K., Hyttinen, M. M., Helminen, H. J., and Prockop, D. J. (2001) Transgenic mice with inactive alleles for procollagen N-proteinase (ADAMTS-2) develop fragile skin and male sterility. *Biochem. J.* **355**, 271–278

4. Hofer, T. P., Frankenberger, M., Mages, J., Lang, R., Meyer, P., Hoffmann, R., Colige, A., and Ziegler-Heitbrock, L. (2008) Tissue-specific induction of ADAMTS2 in monocytes and macrophages by glucocorticoids. *J. Mol. Med. (Berl.)* **86**, 323–332

5. Arning, A., Hiersche, M., Witten, A., Kurlemann, G., Kurnik, K., Manner, D., Stoll, M., and Nowak-Göttl, U. (2012) A genome-wide association study identifies a gene network of ADAMTS genes in the predisposition to pediatric stroke. *Blood* **120**, 5231–5236

6. Goertsches, R., Comabella, M., Navarro, A., Perkal, H., and Montalban, X. (2005) Genetic association between polymorphisms in the ADAMTS14 gene and multiple sclerosis. *J. Neuroimmunol.* **164**, 140–147

7. Poonpet, T., Honsawek, S., Tammachote, N., Kanitnate, S., and Tammachote, R. (2013) ADAMTS14 gene polymorphism associated with knee osteoarthritis in Thai women. *Genet. Mol. Res.* **12**, 5301–5309

8. Rodriguez-Lopez, J., Pombo-Suarez, M., Loughlin, J., Tsezou, A., Blanco, F. J., Meulenbelt, I., Slagboom, P. E., Valdes, A. M., Spector, T. D., Gomez-Reino, J. J., and Gonzalez, A. (2009) Association of a nsSNP in ADAMTS14 to some osteoarthritis phenotypes. *Osteoarthritis Cartilage* **17**, 321–327

9. Lee, C. W., Hwang, I., Park, C. S., Lee, H., Park, D. W., Kang, S. J., Lee, S. W., Kim, Y. H., Park, S. W., and Park, S. J. (2012) Expression of ADAMTS-2, -3, -13, and -14 in culprit coronary lesions in patients with acute myocardial infarction or stable angina. *J. Thromb. Thrombolysis* **33**, 362–370

10. Jeltsch, M., Jha, S. K., Tvorogov, D., Anisimov, A., Leppänen, V. M., Holopainen, T., Kivelä, R., Ortega, S., Kärpanen, T., and Alitalo, K. (2014) CCBE1 enhances lymphangiogenesis via A disintegrin and metalloprotease with thrombospondin motifs-3-mediated vascular endothelial growth factor-C activation. *Circulation* **129**, 1962–1971

11. Kleifeld, O., Doucet, A., auf dem Keller, U., Prudova, A., Schilling, O., Kainthan, R. K., Starr, A. E., Foster, L. J., Kizhakkedathu, J. N., and Overall, C. M. (2010) Isotopic labeling of terminal amines in complex samples identifies protein N-termini and protease cleavage products. *Nat. Biotechnol.* **28**, 281–288

12. Prudova, A., auf dem Keller, U., Butler, G. S., and Overall, C. M. (2010) Multiplex N-terminome analysis of MMP-2 and MMP-9 substrate degradomes by iTRAQ-TAILS quantitative proteomics. *Mol. Cell. Proteomics* **9**, 894–911

13. Jefferson, T., Auf dem Keller, U., Bellac, C., Metz, V. V., Broder, C., Hedrich, J., Ohler, A., Maier, W., Magdolen, V., Sterchi, E., Bond, J. S., Jayakumar, A., Traupe, H., Chalaris, A., Rose-John, S., Pietrzik, C. U., Postina, R., Overall, C. M., and Becker-Pauly, C. (2013) The substrate degradome of meprin metalloproteases reveals an unexpected proteolytic link between meprin β and ADAM10. *Cell. Mol. Life Sci.* **70**, 309–333

14. Fisher, L. W., Stubbs III, J. T., and Young, M. F. (1995) Antisera and cDNA probes to human and certain animal model bone matrix noncollagenous proteins. *Acta Orthop. Scand. Suppl.* **266**, 61–65

15. Moali, C., Font, B., Ruggiero, F., Eichenberger, D., Rousselle, P., François, V., Oldberg, A., Bruckner-Tuderman, L., and Hulmes, D. J. (2005) Substrate-specific modulation of a multisubstrate proteinase. C-terminal processing of fibrillar procollagens is the only BMP-1-dependent activity to be enhanced by PCPE-1. *J. Biol. Chem.* **280**, 24188–24194

16. Colige, A., Ruggiero, F., Vandenberghe, I., Dubail, J., Kesteloot, F., Van Beeumen, J., Beschin, A., Brys, L., Lapière, C. M., and Nusgens, B. (2005) Domains and maturation processes that regulate the activity of ADAMTS-2, a metalloproteinase cleaving the amino-propeptide of fibrillar procollagens types I-III and V. *J. Biol. Chem.* **280**, 34397–34408

17. Colige, A., Sieron, A. L., Li, S. W., Schwarze, U., Petty, E., Wertelecki, W., Wilcox, W., Krakow, D., Cohn, D. H., Reardon, W., Byers, P. H., Lapière, C. M., Prockop, D. J., and Nusgens, B. V. (1999) Human Ehlers-Danlos syndrome type VII C and bovine dermatosparaxis are caused by mutations in the procollagen I N-proteinase gene. *Am. J. Hum. Genet.* **65**, 308–317

18. Kleifeld, O., Doucet, A., Prudova, A., auf dem Keller, U., Gioia, M., Kizhakkedathu, J. N., and Overall, C. M. (2011) Identifying and quantifying proteolytic events and the natural N terminome by terminal amine isotopic labeling of substrates. *Nat. Protoc.* **6**, 1578–1611

19. Vizcaíno, J. A., Deutsch, E. W., Wang, R., Csordas, A., Reisinger, F., Ríos, D., Dianes, J. A., Sun, Z., Farrah, T., Bandeira, N., Binz, P. A., Xenarios, I., Eisenacher, M., Mayer, G., Gatto, L., Campos, A., Chalkley, R. J., Kraus, H. J., Albar, J. P., Martinez-Bartolomé, S., Apweiler, R., Omenn, G. S., Martens, L., Jones, A. R., and Hermjakob, H. (2014) ProteomeXchange provides globally coordinated proteomics data submission and dissemination. *Nat. Biotechnol.* **32**, 223–226

20. Auf dem Keller, U., and Overall, C. M. (2012) CLIPPER: an add-on to the Trans-Proteomic Pipeline for the automated analysis of TAILS N-terminomics data. *Biol. Chem.* **393**, 1477–1483

21. Maere, S., Heymans, K., and Kuiper, M. (2005) BiNGO: a Cytoscape plugin to assess overrepresentation of gene ontology categories in biological networks. *Bioinformatics* **21**, 3448–3449

22. Doucet, A., and Overall, C. M. (2011) Broad coverage identification of multiple proteolytic cleavage site sequences in complex high molecular weight proteins using quantitative proteomics as a complement to edman sequencing. *Mol. Cell. Proteomics* **10**, M110. 003533

23. Delolme, F., Anastasi, C., Alcaraz, L. B., Mendoza, V., Vadon-Le Goff, S., Talantikite, M., Capomaccio, R., Mevaere, J., Fortin, L., Mazzocut, D., Damour, O., Zanella-Cléon, I., Hulmes, D. J., Overall, C. M.,

Valcourt, U., Lopez-Casillas, F., and Moali, C. (2015) Proteolytic control of TGF-β co-receptor activity by BMP-1/tolloid-like proteases revealed by quantitative iTRAQ proteomics. *Cell. Mol. Life Sci.* **72**, 1009–1027

24. Colaert, N., Helsens, K., Martens, L., Vandekerckhove, J., and Gevaert, K. (2009) Improved visualization of protein consensus sequences by iceLogo. *Nat. Methods* **6**, 786–787

25. Lee, E. J., Jo, M., Rho, S. B., Park, K., Yoo, Y. N., Park, J., Chae, M., Zhang, W., and Lee, J. H. (2009) Dkk3, downregulated in cervical cancer, functions as a negative regulator of beta-catenin. *Int. J. Cancer* **124**, 287–297

26. Romero, D., Kawano, Y., Bengoa, N., Walker, M. M., Maltry, N., Niehrs, C., Waxman, J., and Kypta, R. (2013) Downregulation of Dickkopf-3 disrupts prostate acinar morphogenesis through TGF-β/Smad signalling. *J. Cell Sci.* **126**, 1858–1867

27. Ge, G., and Greenspan, D. S. (2006) Developmental roles of the BMP1/TLD metalloproteinases. *Birth Defects Res. C Embryo Today* **78**, 47–68

28. Fish, P. V., Allan, G. A., Bailey, S., Blagg, J., Butt, R., Collis, M. G., Greiling, D., James, K., Kendall, J., McElroy, A., McCleverty, D., Reed, C., Webster, R., and Whitlock, G. A. (2007) Potent and selective nonpeptidic inhibitors of procollagen C-proteinase. *J. Med. Chem.* **50**, 3442–3456

29. Hulmes, D. J., Mould, A. P., and Kessler, E. (1997) The CUB domains of procollagen C-proteinase enhancer control collagen assembly solely by their effect on procollagen C-proteinase/bone morphogenetic protein-1. *Matrix Biol.* **16**, 41–45

30. Das, D. S., Wadhwa, N., Kunj, N., Sarda, K., Pradhan, B. S., and Majumdar, S. S. (2013) Dickkopf homolog 3 (DKK3) plays a crucial role upstream of WNT/β-CATENIN signaling for Sertoli cell mediated regulation of spermatogenesis. *PLoS One* **8**, e63603

31. Dubail, J., Kesteloot, F., Deroanne, C., Motte, P., Lambert, V., Rakic, J. M., Lapière, C., Nusgens, B., and Colige, A. (2010) ADAMTS-2 functions as anti-angiogenic and anti-tumoral molecule independently of its catalytic activity. *Cell. Mol. Life Sci.* **67**, 4213–4232

32. Janssen, L., Dupont, L., Bekhouche, M., Noel, A., Leduc, C., Voz, M., Peers, B., Cataldo, D., Apte, S. S., Dubail, J., and Colige, A. (2015) ADAMTS3 activity is mandatory for embryonic lymphangiogenesis and regulates placental angiogenesis. [E-pub ahead of print] *Angiogenesis*

33. Maurer, L. M., Tomasini-Johansson, B. R., and Mosher, D. F. (2010) Emerging roles of fibronectin in thrombosis. *Thromb. Res.* **125**, 287–291

34. Lohr, K. M., Kurth, C. A., Xie, D. L., Seyer, J. M., and Homandberg, G. A. (1990) The amino-terminal 29- and 72-Kd fragments of fibronectin mediate selective monocyte recruitment. *Blood* **76**, 2117–2124

35. Kawano, Y., Kitaoka, M., Hamada, Y., Walker, M. M., Waxman, J., and Kypta, R. M. (2006) Regulation of prostate cell growth and morphogenesis by Dickkopf-3. *Oncogene* **25**, 6528–6537

36. Sengle, G., Tsutsui, K., Keene, D. R., Tufa, S. F., Carlson, E. J., Charbonneau, N. L., Ono, R. N., Sasaki, T., Wirtz, M. K., Samples, J. R., Fessler, L. I., Fessler, J. H., Sekiguchi, K., Hayflick, S. J., and Sakai, L. Y. (2012) Microenvironmental regulation by fibrillin-1. *PLoS Genet.* **8**, e1002425

37. Bourd-Boittin, K., Bonnier, D., Leyme, A., Mari, B., Tuffery, P., Samson, M., Ezan, F., Baffet, G., and Theret, N. (2011) Protease profiling of liver fibrosis reveals the ADAM metallopeptidase with thrombospondin type 1 motif, 1 as a central activator of transforming growth factor beta. *Hepatology* **54**, 2173–2184

38. Kesteloot, F., Desmoulière, A., Leclercq, I., Thiry, M., Arrese, J. E., Prockop, D. J., Lapière, C. M., Nusgens, B. V., and Colige, A. (2007) ADAM metallopeptidase with thrombospondin type 1 motif 2 inactivation reduces the extent and stability of carbon tetrachloride-induced hepatic fibrosis in mice. *Hepatology* **46**, 1620–1631

39. Crawford, S. E., Stellmach, V., Murphy-Ullrich, J. E., Ribeiro, S. M., Lawler, J., Hynes, R. O., Boivin, G. P., and Bouck, N. (1998) Thrombospondin-1 is a major activator of TGF-beta1 in vivo. *Cell* **93**, 1159–1170

40. Murphy-Ullrich, J. E., and Poczatek, M. (2000) Activation of latent TGF-beta by thrombospondin-1: mechanisms and physiology. *Cytokine Growth Factor Rev.* **11**, 59–69

41. Esparza-Lopez, J., Montiel, J. L., Vilchis-Landeros, M. M., Okadome, T., Miyazono, K., and López-Casillas, F. (2001) Ligand binding and functional properties of betaglycan, a co-receptor of the transforming growth factor-beta superfamily. Specialized binding regions for transforming growth factor-beta and inhibin A. *J. Biol. Chem.* **276**, 14588–14596

42. López-Casillas, F., Wrana, J. L., and Massagué, J. (1993) Betaglycan presents ligand to the TGF beta signaling receptor. *Cell* **73**, 1435–1444

43. Velasco-Loyden, G., Arribas, J., and López-Casillas, F. (2004) The shedding of betaglycan is regulated by pervanadate and mediated by membrane type matrix metalloprotease-1. *J. Biol. Chem.* **279**, 7721–7733

44. Boivin, W. A., Shackleford, M., Vanden Hoek, A., Zhao, H., Hackett, T. L., Knight, D. A., and Granville, D. J. (2012) Granzyme B cleaves decorin, biglycan and soluble betaglycan, releasing active transforming growth factor-β1. *PLoS One* **7**, e33163

45. Mendoza, V., Vilchis-Landeros, M. M., Mendoza-Hernández, G., Huang, T., Villarreal, M. M., Hinck, A. P., López-Casillas, F., and Montiel, J. L. (2009) Betaglycan has two independent domains required for high affinity TGF-beta binding: proteolytic cleavage separates the domains and inactivates the neutralizing activity of the soluble receptor. *Biochemistry* **48**, 11755–11765

46. Kirkbride, K. C., Townsend, T. A., Bruinsma, M. W., Barnett, J. V., and Blobe, G. C. (2008) Bone morphogenetic proteins signal through the transforming growth factor-beta type III receptor. *J. Biol. Chem.* **283**, 7628–7637

47. Wang, W. M., Lee, S., Steiglitz, B. M., Scott, I. C., Lebares, C. C., Allen, M. L., Brenner, M. C., Takahara, K., and Greenspan, D. S. (2003) Transforming growth factor-beta induces secretion of activated ADAMTS-2. A procollagen III N-proteinase. *J. Biol. Chem.* **278**, 19549–19557

48. Verrecchia, F., and Mauviel, A. (2002) Transforming growth factor-beta signaling through the Smad pathway: role in extracellular matrix gene expression and regulation. *J. Invest. Dermatol.* **118**, 211–215

49. Verrecchia, F., and Mauviel, A. (2007) Transforming growth factor-beta and fibrosis. *World J. Gastroenterol.* **13**, 3056–3062